

# Cobalt Catalysis in the Gas Phase: Experimental Characterization of Cobalt(I) Complexes as Intermediates in Regioselective Diels–Alder Reactions

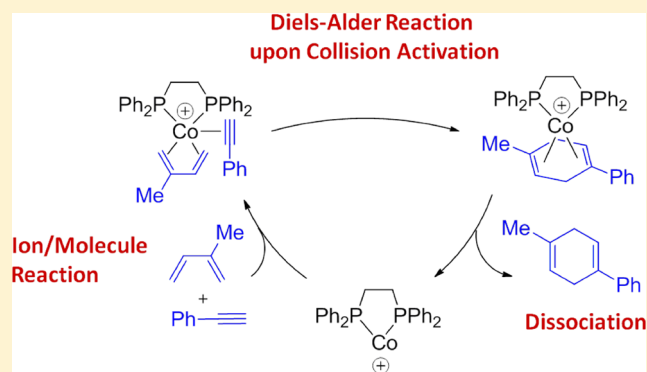
Lukas Fiebig,<sup>†</sup> Julian Kuttner,<sup>‡</sup> Gerhard Hilt,<sup>‡</sup> Martin C. Schwarzer,<sup>‡</sup> Gernot Frenking,<sup>‡</sup> Hans-Günther Schmalz,<sup>†</sup> and Mathias Schäfer<sup>\*,†</sup>

<sup>†</sup>Department of Chemistry, University of Cologne, Greinstraße 4, 50939 Köln, Germany

<sup>‡</sup>Fachbereich Chemie, Philipps University of Marburg, Hans-Meerwein-Straße, 35043 Marburg, Germany

**S** Supporting Information

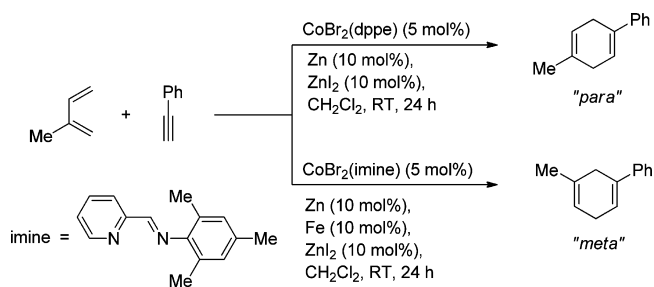
**ABSTRACT:** In situ-formed cobalt(I) complexes are proposed to act as efficient catalysts in regioselective Diels–Alder reactions of unactivated substrates such as 1,3-dienes and alkynes. We report the first experimental evidence for the in situ reduction of  $\text{CoBr}_2(\text{dppe})$  [ $\text{dppe} = 1,2\text{-bis}(\text{diphenylphosphino})\text{ethane}$ ] by  $\text{Zn}/\text{ZnI}_2$  to  $[\text{Co}(\text{I})(\text{dppe})]^+$  by means of electrospray  $\text{MS}^n$  experiments. Additionally, the reactivities of  $\text{Co}(\text{II})$  and  $\text{Co}(\text{I})$   $\text{dppe}$  complexes toward the Diels–Alder substrates isoprene and phenylacetylene were probed in gas-phase ion/molecule reactions (IMRs). Isoprene and phenylacetylene were introduced into the mass spectrometer via the buffer gas flow of a linear ion trap. The IMR experiments revealed a significantly higher substrate affinity of  $[\text{Co}(\text{I})(\text{dppe})]^+$  compared with  $[\text{Co}(\text{II})\text{Br}(\text{dppe})]^+$ . Furthermore, the central intermediate of the solution-phase cobalt-catalyzed Diels–Alder reaction,  $[\text{Co}(\text{I})(\text{dppe})(\text{isoprene})(\text{phenylacetylene})]^+$ , could be generated via IMR and examined in the gas phase. Collision activation of this complex ion delivered evidence for the gas-phase reaction of isoprene with phenylacetylene in the coordination sphere of the cobalt ion. The experimental findings are consistent with the results of quantum-chemical calculations on all of the observed  $\text{Co}(\text{I})$   $\text{dppe}$  complex ions. The results constitute strong analytical evidence for the formation and importance of different cobalt(I) species in regioselective Diels–Alder reactions of unactivated substrates and identify  $[\text{Co}(\text{I})(\text{dppe})]^+$  as the active Diels–Alder catalyst.



## 1. INTRODUCTION

Since its discovery in 1928, the Diels–Alder reaction has become one of the most valuable tools in the synthesis of natural products and other complex organic molecules.<sup>1–3</sup> The limited reactivity of certain “unactivated” starting materials in Diels–Alder reactions can be overcome by the application of transition-metal catalysts, in particular when alkynes are used as dienophiles.<sup>4–11</sup> A remarkably efficient catalyst generated from  $\text{CoBr}_2(\text{ligand})$  by in situ reduction with zinc and zinc iodide was found to efficiently catalyze the formal Diels–Alder reaction of isoprene and phenylacetylene. Interestingly, the “*para*” product was obtained with high regioselectivity when the ligand was 1,2-bis(diphenylphosphino)ethane ( $\text{dppe}$ ), while the “*meta*” product was selectively formed with the imine ligand (*E*)-2,4,6-trimethyl-*N*-(pyridine-2-ylmethylene)aniline (Scheme 1).<sup>8</sup> Besides this, the catalyst obtained from  $\text{CoBr}_2(\text{dppe})$  by reduction with  $\text{Zn}/\text{ZnI}_2$  was shown to efficiently catalyze also other transformations, including 1,4-hydrovinylation,<sup>12–14</sup>  $[2 + 2 + 2]$  cycloadditions,<sup>15,16</sup> Alder-en reactions,<sup>17–19</sup>  $[4 + 2 + 2]$  cycloadditions,<sup>20</sup>  $[2 + 2]$  cycloadditions,<sup>21</sup> homo-Diels–Alder reactions,<sup>22,23</sup> isomeriza-

### Scheme 1. Regioselective Cobalt-Catalyzed Diels–Alder Reaction of Phenylacetylene and Isoprene<sup>8</sup>



tions of 1,3-dienes,<sup>24</sup> Glaser couplings,<sup>25</sup> and benzannulations of conjugated enynes.<sup>26</sup>

The addition of both zinc and zinc iodide is of vital importance for the generation of the active cobalt catalyst for the regioselective Diels–Alder reaction of 1,3-dienes with

Received: September 10, 2013

Published: September 17, 2013

alkynes. This suggests that the neutral  $\text{CoBr}_2(\text{ligand})$  complex is initially reduced to a  $\text{Co(I)}$  species while the remaining halide ion is abstracted by the Lewis acid  $\text{ZnI}_2$ . The resulting cationic  $[\text{Co(I)}(\text{ligand})]^{+}$  complex is expected to act as the catalytically active species.<sup>27</sup> According to Hilt and Frenking, the catalytic cycle is suggested to start from the diamagnetic 18 VE complex  $[\text{Co(I)}(\text{ligand})(\text{solvent})_3]^{+}$ , which sequentially exchanges solvent molecules for the Diels–Alder substrates to generate the  $[\text{Co(I)}(\text{ligand})(\text{diene})(\text{alkyne})]^{+}$  complex, the actual precursor for the C–C bond-forming steps (Figure 1).<sup>27</sup> Extensive

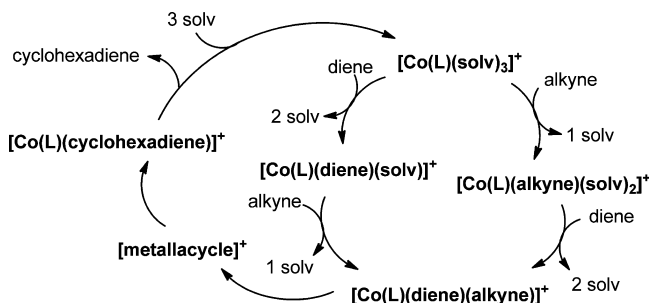


**Figure 1.** Postulated catalytic cycle of the  $\text{Co(I)}$ -catalyzed Diels–Alder reaction.<sup>27</sup>

theoretical investigation of the mechanism of the cobalt-mediated formal Diels–Alder reaction of isoprene with phenylacetylene indicates that the cycloaddition actually proceeds in a two-step fashion. First, oxidative cyclization (as the rate-determining step) yields a metallacyclic intermediate, which then undergoes reductive elimination. Finally, the Diels–Alder product (i.e., the 1,4-cyclohexadiene) is released to regenerate the  $[\text{Co(I)}(\text{ligand})]^{+}$  catalyst. It was shown that the formation of the metallacycle (i.e., the formation of the first C–C bond) is not only the rate-limiting step but also the regioselectivity-determining step. Thus, the computations suggest that the regioselectivity of the cobalt-catalyzed Diels–Alder reaction is kinetically controlled and ultimately determined by steric interactions of the bidentate ligands. More precisely, the distance between the carbon atoms involved in the initial C–C bond formation and the relative energies of the four possible conformations of the  $[\text{Co(I)}(\text{ligand})(\text{isoprene})(\text{phenylacetylene})]^{+}$  intermediate govern the regioselectivity.<sup>27</sup>

Apart from the theoretical efforts, spectroscopic methods have also been applied to elucidate the catalytic cycles of metal-mediated transformations experimentally. In this challenging task, electrospray ionization mass spectrometry (ESI-MS)<sup>28–30</sup> in combination with tandem  $\text{MS}^{31}$  represents a powerful and versatile approach, as even labile and transient species can be transferred intact into the mass spectrometer, given that soft and gentle ionization and phase-transfer conditions are selected. In doing so, all kinds of ionic (or previously charge-tagged) reactive intermediates can be directly identified out of very complex reaction solutions, and interesting features of the reaction under examination (such as the concentrations of starting materials, intermediates, and products) can be simultaneously monitored.<sup>32–45</sup> Furthermore, a quadrupole or magnetic ion trap mass spectrometer can be used as a versatile reaction chamber for the examination of intrinsic structure–reactivity relationships of ionic organometallic complexes in vacuo without the influence of solvent molecules and counterions, as documented by numerous studies.<sup>46–49</sup> Either

sequential  $\text{MS}^n$  product ion experiments of selected precursor ions by means of collision-induced dissociation (CID) can be conducted or ion/molecule reactions (IMRs) between an ionic organometallic reagent and a neutral substrate can be performed. This way, it is possible to investigate the nature of the coordination sphere of transition-metal complexes<sup>50–52</sup> and the kinetics of adduct ion formation within complexes bearing different ligands.<sup>53–55</sup> Complete catalytic cycles have thus been examined,<sup>56,57</sup> and the technique has been used to screen the reactivities of potential catalysts in polymerization reactions.<sup>58,59</sup>

In the present study, we probed relevant intermediates of the cobalt-catalyzed Diels–Alder reaction (Scheme 1) by means of ESI-MS,  $\text{MS}^n$  product ion experiments, and gas-phase IMRs in an MS instrument that is also able to measure exact ion masses. The experiments were performed using the established catalyst system [generated from  $\text{CoBr}_2(\text{dppe})$  by reaction with  $\text{Zn}/\text{ZnI}_2$  in THF] and isoprene and phenylacetylene as the substrates. We report the first experimental evidence for the in situ formation of the until now only postulated cationic  $\text{Co(I)}$  complex  $[\text{Co(I)}(\text{dppe})]^{+}$ . Additionally, the reactivities of cationic  $\text{Co(II)}$  and  $\text{Co(I)}$  intermediates toward the Diels–Alder substrates were studied in respective gas-phase IMRs, which even allowed us to identify and characterize the complex ion  $[\text{Co(I)}(\text{dppe})(\text{isoprene})(\text{phenylacetylene})]^{+}$  (Figure 1). Finally, we report extensive experimental evidence for the transformation of  $[\text{Co(I)}(\text{dppe})(\text{isoprene})(\text{phenylacetylene})]^{+}$  into  $[\text{Co(I)}(\text{dppe})(1\text{-methyl-4-phenylcyclohexadiene})]^{+}$  and the release of the Diels–Alder product upon collision activation in the gas phase. The conclusions of the experimental study are furthermore supported by quantum-chemical computations.

## 2. RESULTS AND DISCUSSION

As a starting point of the study, a  $10^{-5}$  M solution of  $\text{CoBr}_2(\text{dppe})$  in acetonitrile was analyzed by (+)ESI-MS. The respective spectrum presented in Figure 2a exhibits characteristic signals of the ionic  $\text{Co(II)}$  species  $[\text{Co}^{79}\text{Br}(\text{dppe})]^{+}$  (**1**) ( $m/z$  536) along with other ionic  $\text{Co(II)}$  complexes decorated with a solvent  $\text{CH}_3\text{CN}$  molecule or an additional dppe ligand  $[\text{Co}^{79}\text{Br}(\text{dppe})_2]^{+}$  ( $m/z$  934). The identity of  $\text{Co(II)}$  complex ion **1** was reliably confirmed by the exact ion mass, by its characteristic isotope distribution (which clearly evidences the presence of a bromine atom; Figure 2a inset), and furthermore by an indicative fragmentation pattern in an  $\text{MS}^2$  product ion experiment [Figure S2 in the Supporting Information (SI)]. The ions at  $m/z$  293, 321, 352, and 428 represent fragment ions of **1**, as they also appear as product ions in the CID experiment of **1** (Figure S1 in the SI).

After (+)ESI-MS characterization of a  $\text{CoBr}_2(\text{dppe})$  solution and  $\text{MS}^n$  analysis of  $[\text{Co(II)}\text{Br}(\text{dppe})]^{+}$  complex ion **1**, the role of the reducing agent ( $\text{Zn}/\text{ZnI}_2$ ) was probed next. To test the postulated in situ reduction<sup>27</sup> of  $\text{Co(II)}\text{Br}_2(\text{dppe})$  to a respective  $\text{Co(I)}$  complex, a solution of  $\text{CoBr}_2(\text{dppe})$  was treated with zinc powder (2 equiv) and zinc iodide (2 equiv) in THF under an inert gas atmosphere according to the established experimental protocol of Hilt et al.<sup>8,60</sup> The (+)ESI-MS spectrum of this reaction solution is presented in Figure 2b. The signal at  $m/z$  457 is assigned to the  $\text{Co(I)}$  complex ion  $[\text{Co(I)}(\text{dppe})]^{+}$  (**2**). The isotope pattern of that ion confirms the absence of any bromine or zinc atom and is consistent with the computed isotopic distribution of the proposed  $\text{Co(I)}$  complex **2**. Additionally, the fragmentation pattern observed in an  $\text{MS}^2$  product ion experiment on the ion

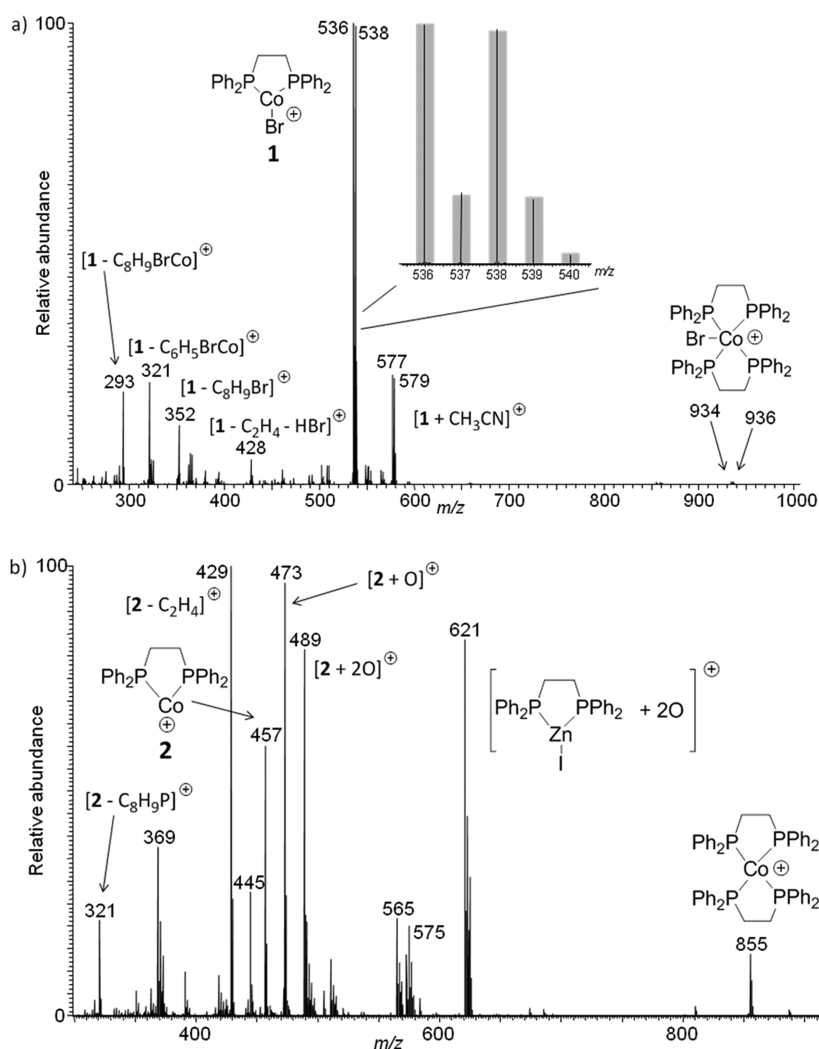


**Figure 2.** (a) (+)ESI-MS spectrum of a  $10^{-5}$  M solution of  $\text{CoBr}_2(\text{dppe})$  in acetonitrile. The structure assignment of Co(II) complex ion **1** ( $m/z$  536) was confirmed by the measured exact ion mass and (inset) the characteristic isotope distribution, which matches the computed isotopic pattern. (b) (+)ESI-MS spectrum of a reaction mixture of  $\text{CoBr}_2(\text{dppe})$ , Zn, and  $\text{ZnI}_2$  in THF, representing typical reaction conditions for the catalytic Diels–Alder protocol before the addition of substrates.<sup>8,60</sup>

at  $m/z$  457 supports this structure assignment (Figure S2 in the SI). The observed set of product ions formed, inter alia, by the loss of  $\text{C}_2\text{H}_4$  and  $\text{C}_6\text{H}_6$  can be attributed to the fragmentation of the dppe ligand of **2**. Aside from the Co(I) complex ion **2**, Co(I) oxygen adduct species,<sup>61</sup> ionic Zn complexes, and in-source fragment ions can be found in the mass spectrum, as Figure 2b illustrates.

Following the detection and identification of the complex ions  $[\text{Co}(\text{II})\text{Br}(\text{dppe})]^+$  (**1**) and  $[\text{Co}(\text{I})(\text{dppe})]^+$  (**2**), we turned our attention to the gas-phase reactivities of these cobalt complex ions toward the Diels–Alder substrates isoprene and phenylacetylene. For this purpose, gas-phase IMRs were performed by metered introduction of the neutral substrates into the helium buffer gas flow of the linear ion trap (LTQ) according to the instrumental modification established by Gronert<sup>47</sup> and O’Hair.<sup>56,62</sup> Figure 3 presents relative precursor ion intensities as functions of the reaction time for the IMRs of isoprene with (a)  $[\text{Co}(\text{II})^{79}\text{Br}(\text{dppe})]^+$  (**1**) and (b)  $[\text{Co}(\text{I})(\text{dppe})]^+$  (**2**). The outcomes of the IMR experiments document that the Co(I) complex ion  $[\text{Co}(\text{I})(\text{dppe})]^+$  (**2**) has a stronger affinity to form the adduct  $[\text{Co}(\text{I})(\text{dppe})(\text{isoprene})]^+$  (**4**) than the respective Co(II) complex.

Analogous results were found in the IMRs of both Co complex ions with phenylacetylene. In this case, however,  $[\text{Co}(\text{II})^{79}\text{Br}(\text{dppe})]^+$  (**1**) was found to be completely unreactive toward the alkyne substrate, as no adduct formation could be observed at reaction times up to 10 s (Figure S3 in the SI). These findings are in line with the results of quantum-chemical calculations showing a significantly higher formation enthalpy for  $[\text{Co}(\text{I})(\text{dppe})(\text{substrate})]^+$  relative to  $[\text{Co}(\text{II})\text{Br}(\text{dppe})(\text{substrate})]^+$  (Figure S4 and Table S1 in the SI).<sup>63</sup>

In the next step, IMRs of the Co complex ions with both substrates present in the He buffer gas were conducted by infusing an equimolar mixture of isoprene and phenylacetylene into the He line. When  $[\text{Co}(\text{II})^{79}\text{Br}(\text{dppe})]^+$  (**1**) was isolated in the LTQ and reacted with isoprene and phenylacetylene for up to 10 s, only the isoprene adduct ion  $[\text{Co}(\text{II})^{79}\text{Br}(\text{dppe})(\text{isoprene})]^+$  (**3**) ( $m/z$  604) was observed (Figure 4a). In contrast, LTQ selection of  $[\text{Co}(\text{I})(\text{dppe})]^+$  (**2**) and reaction with isoprene and phenylacetylene for 300 ms yielded the adduct ions  $[\text{Co}(\text{I})(\text{dppe})(\text{isoprene})]^+$  (**4**) ( $m/z$  525),  $[\text{Co}(\text{I})(\text{dppe})(\text{phenylacetylene})]^+$  (**5**) ( $m/z$  559), and  $[\text{Co}(\text{I})(\text{dppe})(\text{isoprene})(\text{phenylacetylene})]^+$  (**6**) ( $m/z$  627), as shown in Figure 4b. When collision activated, the adduct ions **4** and **5**

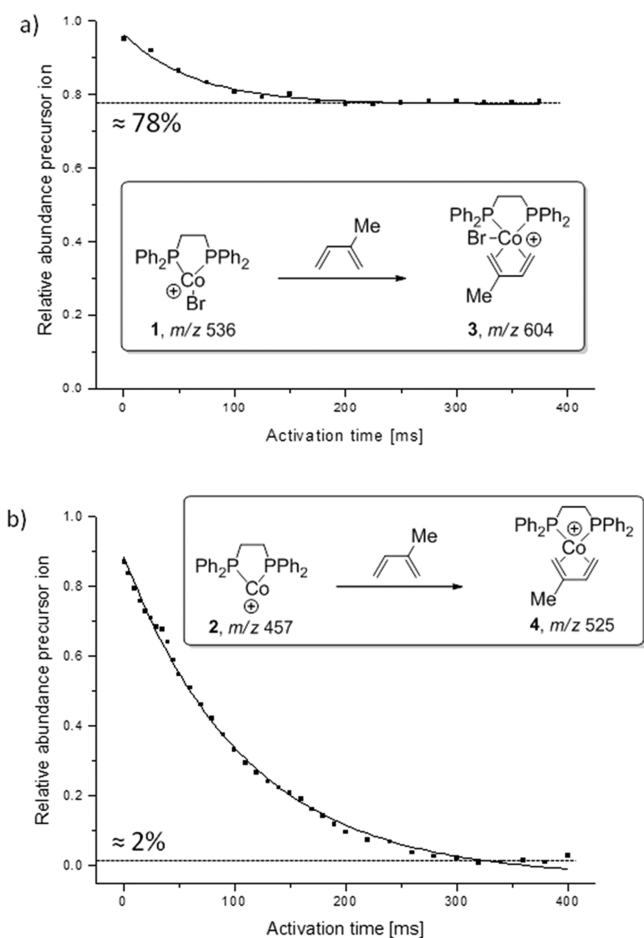


**Figure 3.** MS data for the IMRs of isoprene with (a)  $[\text{Co}(\text{II})^{79}\text{Br}(\text{dppe})]^+$  (**1**) and (b)  $[\text{Co}(\text{I})(\text{dppe})]^+$  (**2**), which deliver exclusively the depicted product ions. In each panel, the relative precursor ion intensity is shown as a function of the reaction time. The IMRs of **1** and **2** with isoprene are shown in the insets of (a) and (b), respectively.

lose the olefin and alkyne ligand, respectively. In addition, the formation of a new adduct ion with the other substrate in each case is observed (Figure S5 in the SI). These experimental findings strongly support the postulate that a Co(I) complex acts as the catalytically active species in this type of catalytic Diels–Alder reaction as follows: first, the poor gas-phase affinity of  $[\text{Co}(\text{II})^{79}\text{Br}(\text{dppe})]^+$  (**1**) toward isoprene and phenylacetylene has been evidenced, and second, all three proposed intermediary cobalt–substrate complexes could be formed and characterized only with the Co(I) precursor complex by gas-phase IMRs.<sup>27</sup>

Careful isolation of the complex ion  $[\text{Co}(\text{I})(\text{dppe})(\text{isoprene})]^+$  (**4**) formed by IMR followed by another IMR step with phenylacetylene yielded the complex ion  $[\text{Co}(\text{I})(\text{dppe})(\text{isoprene})(\text{phenylacetylene})]^+$  (**6**) with sufficiently high abundance to allow precursor ion selection and activation in a subsequent product ion experiment (Scheme 2). The product ion spectra of  $[\text{Co}(\text{I})(\text{dppe})(\text{isoprene})(\text{phenylacetylene})]^+$  (**6**) at different normalized collision energies (NCEs) are presented in Figure 5.<sup>64–66</sup> The precursor ion at  $m/z$  627 starts to disintegrate at an NCE of 13 (Figure 5b). In all of the CID experiments with NCE values of 13 and higher (Figure 5b–d), only the product ions **2**, **4**, and **5** were generated, and we found no evidence of the alternative retro-Diels–Alder pathway,

which would give propyne and 2-phenyl-1,3-butadiene attached to **2**. In all three spectra (Figure 5b–d) the Co(I) complex ion  $[\text{Co}(\text{I})(\text{dppe})]^+$  (**2**) appears with the highest abundance of the product ions formed. Accordingly, the loss of a single ligand, either phenylacetylene or isoprene, is less pronounced than the simultaneous loss of both substrates leading to product ion **2** at  $m/z$  457. The concerted neutral loss of both ligands (i.e., a loss of 170 Da) correlates with the Diels–Alder product of isoprene and phenylacetylene, namely, a (methyl)(phenyl)cyclohexadiene ( $\text{C}_{13}\text{H}_{14}$ ). However, an unambiguous distinction between the loss of 170 Da in a single step and the sequential loss of isoprene and phenylacetylene (which also formally adds up to 170 Da) is not possible on the basis of the mass difference alone (Scheme 2).

Actually, we advocate the elimination of a single  $\text{C}_{13}\text{H}_{14}$  molecule, that is, the release of the neutral Diels–Alder product.<sup>67,68</sup> This assumption is based on the following arguments. First, CID experiments in quadrupole ion traps (QITs) are achieved by resonant activation of the precursor ion, and thus, ions formed by primary fragmentation reactions are not further activated but instead cooled for detection.<sup>69–71</sup> Hence, secondary fragmentation reactions only take place intentionally in broadband activation experiments<sup>70,71</sup> or at high-end collision energies (complete depletion of the precursor ion).<sup>72,73</sup> However, Figure 5 exhibits the formal loss of both substrates leading to the predominant product ion  $[\text{Co}(\text{I})(\text{dppe})]^+$  (**2**) ( $m/z$  457) even at minimum collision energies (with no broadband activation applied), pointing toward the joint loss of  $\text{C}_{13}\text{H}_{14}$  in a single step.

Second, it cannot be excluded that a significant fraction of the ions **4** and **5** found in Figure 5b–d are actually not direct product ions of the collision-activated precursor ion. It is rather likely that ions **4** and **5** are subsequently formed by IMR of the initially generated product ion  $[\text{Co}(\text{I})(\text{dppe})]^+$  (**2**), as isoprene and phenylacetylene are still present in the atmosphere of the LTQ (Scheme 2). This conclusion was further probed by a control experiment in which product ion **2** ( $m/z$  457) formed by CID of the ion at  $m/z$  627 (**6/6'**) was reselected for IMR. The adduct ions **4** and **5** were formed by IMR and found in an abundance ratio similar to that observed in Figure 5b–d. This experimental finding strongly supports our assumption (Figure S6b in the SI). Secondary adduct formation reactions were also observed in the CID experiments on  $[\text{Co}(\text{I})(\text{dppe})(\text{isoprene})]^+$  (**4**) ( $m/z$  525) and  $[\text{Co}(\text{I})(\text{dppe})(\text{phenylacetylene})]^+$  (**5**) ( $m/z$  559) (Figure S5 in the SI). In these control experiments, the complementary complex ions **5** and **4** were formed by secondary IMR of the product ion  $[\text{Co}(\text{I})(\text{dppe})]^+$  (**2**) with gaseous phenylacetylene and isoprene, both of which were present in the LTQ. However, we note a slight difference in the signal abundance ratios of product ions **4** and **5** produced by IMR of complex ion **2** (Figure 4b) and in the CID experiment of the complex ion at  $m/z$  627 (**6/6'**) (Figure 5b–d). However, control experiments documented that the ratios of the ions **4** and **5** formed either by IMR of **2** at  $m/z$  457 (Figure 4b) or by subsequent IMR after CID of **6** at  $m/z$  627 (Figure 5b–d) are very sensitive to the actual experimental conditions and vary around a ratio of 1:1.

To scrutinize our assumptions based on the experimental findings, we conducted an extensive computational analysis of all ions relevant for the understanding of the investigated Diels–Alder reaction in the gas phase. The structures and relative stabilities ( $\Delta E$  and  $\Delta G_{298\text{K}}$ ) of the Co(I) complex ions were ascertained. In particular, the ion structures of the

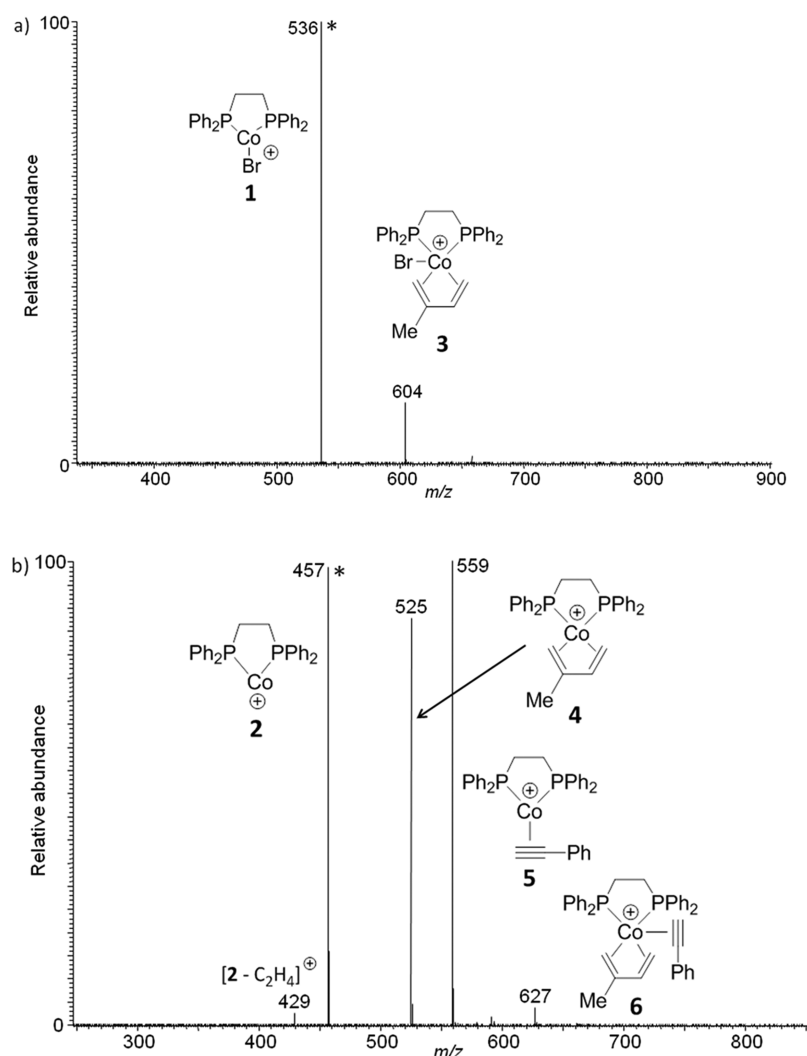
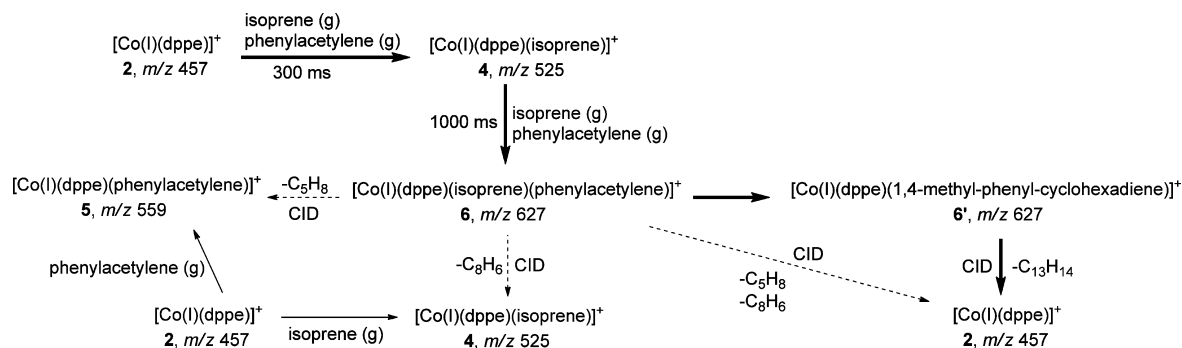


**Figure 4.** MS data for the IMRs of an equimolar mixture of isoprene and phenylacetylene with (a)  $[\text{Co}(\text{II})^{79}\text{Br}(\text{dppe})]^+$  (1) and (b)  $[\text{Co}(\text{I})(\text{dppe})]^+$  (2) at a reaction time of 300 ms (also see Figure S6a in the SI). The precursor ions selected for IMR are marked with asterisks. The low-abundance signal at  $m/z$  429 in (b) corresponds to a fragment ion of precursor ion 2 (loss of  $\text{C}_2\text{H}_4$ ). The molecular structure of the IMR product ion 6 at  $m/z$  627 has not been fully verified to date (see the text for discussion).

**Scheme 2. IMR of  $[\text{Co}(\text{I})(\text{dppe})]^+$  (2) with Isoprene and Phenylacetylene and Subsequent CID Experiment Using the Complex Ion at  $m/z$  627<sup>a</sup>**



<sup>a</sup>The  $\text{Co}(\text{I})$  complex ion at  $m/z$  627 is either  $[\text{Co}(\text{I})(\text{dppe})(\text{isoprene})(\text{phenylacetylene})]^+$  (6) or  $[\text{Co}(\text{I})(\text{dppe})(1\text{-methyl-4-phenylcyclohexadiene})]^+$  (6').

complexes  $[\text{Co}(\text{I})(\text{dppe})]^+$  (2),  $[\text{Co}(\text{I})(\text{dppe})(\text{isoprene})]^+$  (4), and  $[\text{Co}(\text{I})(\text{dppe})(\text{phenylacetylene})]^+$  (5), all relevant for the performed IMR experiments, were examined (Figure S4 and Table S1 in the SI). Additionally, the complex ion  $[\text{Co}(\text{I})$

$(\text{dppe})(\text{isoprene})(\text{phenylacetylene})]^+$  (6) and its isobaric isomer containing the Diels–Alder product attached to the  $\text{Co}(\text{I})$  cation,  $[\text{Co}(\text{I})(\text{dppe})(1\text{-methyl-4-phenylcyclohexadiene})]^+$  (6'), were investigated (Figure 6 and Table S1 in

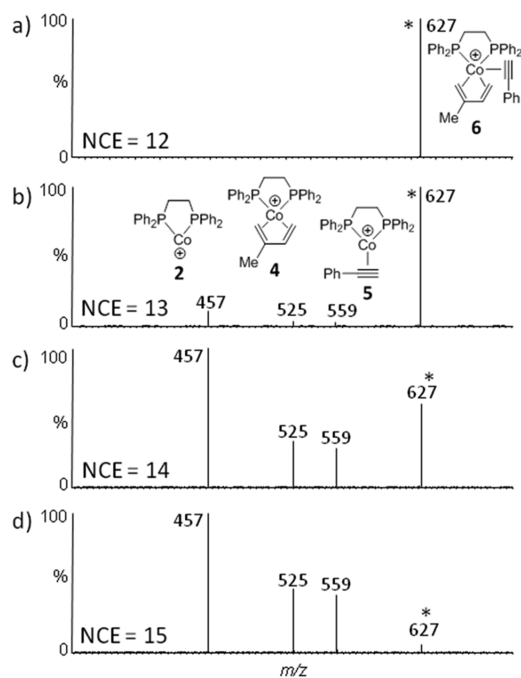


**Figure 5.** Product ion experiments of the complex ion  $[\text{Co}(\text{I})(\text{dppe})\text{-(isoprene)(phenylacetylene)}]^+$  (**6**) (*m/z* 627) at different normalized collision energies (NCEs). The precursor ion is marked with an asterisk.

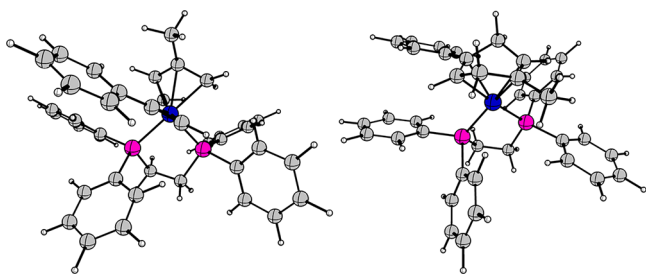


**Figure 6.** Calculated structures of the cobalt complex ions **6** (left) and **6'** (right). Cobalt atoms are shown in blue and phosphorus atoms in pink.

the SI). The computed relative electronic energies ( $\Delta E$ ) and free energies ( $\Delta G_{298\text{K}}$ ) for the set of gas-phase reactions are presented in Scheme 3. It should be noted that the  $\Delta E$  and  $\Delta G_{298\text{K}}$  values document only the relative stabilities of the computed ion structures and are exclusively used in this regard to estimate the probabilities of competing reaction pathways. The computational determination of transition states and related activation energy barriers of the various reaction pathways, although certainly desirable, was far too costly because of the size and complexity of the ion structures.

However, calculations from an earlier contribution suggested an activation free energy barrier of only 11–12 kcal/mol for the Diels–Alder reaction of isoprene with phenylacetylene in the respective Co(I) dppe complex, that is, the interconversion of complex ion **6** into the complex ion  $[\text{Co}(\text{I})(\text{dppe})(1\text{-methyl-4-phenylcyclohexadiene})]^+$  (**6'**).<sup>27,74</sup> In view of this piece of information, it seems very likely that the collision activation of complex **6** provides enough internal energy for the Diels–Alder reaction to proceed. Furthermore, theory predicts that the simultaneous release of isoprene and phenylacetylene from complex ion **6** is energetically significantly more costly, and

therefore more unlikely, than (i) the release of the Diels–Alder product  $\text{C}_{13}\text{H}_{14}$  from Co(I) complex ion **6'** and (ii) the separate loss of either isoprene or phenylacetylene from complex **6**, as Scheme 3 illustrates. Additionally, a rough estimation of the gas-phase equilibrium yields a minimum enthalpy of association of about 25 kcal/mol for a complex formed by an IMR association reaction under the given circumstances to be stable in a quadrupole ion trap.<sup>75,76</sup>

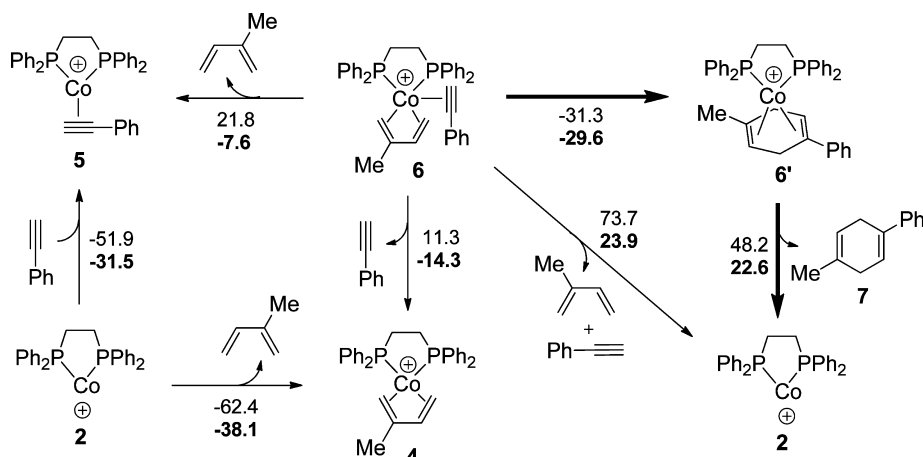
Accordingly, the computed energy differences even point toward an effective and direct Diels–Alder reaction to give the cyclohexadiene complex **6'** from complex ion **6**. Hence, the experimental finding that product ion **2** dominates the product ion spectra of the precursor ion **6** or **6'** at all NCEs (Figure 5b–d) provides clear evidence for the gas-phase Diels–Alder reaction (formation of complex **6'**) with subsequent release of the product, 1-methyl-4-phenylcyclohexadiene (**7**). Thus, the experimental results are in full agreement with theory: either directly or upon collision activation of complex **6**, the formal Diels–Alder reaction leading to complex **6'** is initiated, and the release of **7** ultimately yields  $[\text{Co}(\text{I})(\text{dppe})]^+$  (**2**). The observation of complex ions **4** and **5** can be rationalized by energetically favored IMRs of ion **2** with the neutral Diels–Alder substrates available in the gas phase (reaction pathways with solid arrows in Scheme 2). The solution-phase regioselectivity of the  $[\text{Co}(\text{I})(\text{dppe})]^+$  catalyst, which favors the formation of the “*para*” product **7**, is not yet proven in the gas phase, but theory suggests that the complex ion  $[\text{Co}(\text{I})(\text{dppe})(1\text{-methyl-4-phenylcyclohexadiene})]^+$  (**6'**) is 0.9 kcal/mol lower in energy than the isomeric complex ion  $[\text{Co}(\text{I})(\text{dppe})(1\text{-methyl-3-phenylcyclohexadiene})]^+$  (**6''**) (see Figure S8 in the SI). Additional gas-phase studies to probe the reactivity and regioselectivity of the  $[\text{Co}(\text{I})(\text{imine})]^+$  catalyst system (Scheme 1), which selectively promotes the formation of the “*meta*” Diels–Alder product 1-methyl-3-phenylcyclohexadiene in solution, are currently underway.

### 3. CONCLUSIONS

Typical reaction solutions for cobalt-catalyzed regioselective Diels–Alder reactions, enabling the in situ reduction of  $\text{Co}(\text{II})\text{Br}_2(\text{dppe})$  with  $\text{Zn}/\text{ZnI}_2$ , were analyzed by (+)ESI-MS. The cobalt(dppe) complex ions  $[\text{Co}(\text{II})\text{Br}(\text{dppe})]^+$  (**1**) and the until now only postulated transient Co(I) species  $[\text{Co}(\text{I})(\text{dppe})]^+$  (**2**) could be initially detected and unambiguously characterized. Furthermore, the intrinsic reactivities of cobalt complex ions **1** and **2** toward the exemplary Diels–Alder substrates isoprene and phenylacetylene were examined by gas-phase IMRs. These experiments evidenced a substantially reduced affinity of the Co(II) species **1** toward isoprene and phenylacetylene relative to the complex ion  $[\text{Co}(\text{I})(\text{dppe})]^+$  (**2**).

Additionally, solvent-free Co(I)(dppe)–substrate complexes that have been proposed to be key intermediates in the cobalt-catalyzed Diels–Alder reaction mechanism could be generated in the gas phase by carefully conducted IMRs and were fully characterized by exact ion mass measurements, the analysis of isotopic distributions, and conclusive product ion experiments. Moreover, the Co(I) complex  $[\text{Co}(\text{I})(\text{dppe})(\text{isoprene})(\text{phenylacetylene})]^+$  (**6**), proposed to be the mechanistic starting complex of this type of Diels–Alder reaction, could be generated and further examined in CID experiments. Upon collision activation, complex **6** showed the preferred loss of a  $\text{C}_{13}\text{H}_{14}$  hydrocarbon unit, a strong indication of the completion of the Diels–Alder reaction in the gas phase, thereby

Scheme 3. Calculated Relative Electronic Energies ( $\Delta E$ ) and Free Energies ( $\Delta G_{298K}$ , shown in bold) for the CID Reactions of the Complex Ions  $[\text{Co(I)(dppe)(isoprene)(phenylacetylene)}]^+$  (**6**) and  $[\text{Co(I)(dppe)(1-methyl-4-phenylcyclohexadiene)}]^+$  (**6'**)<sup>a</sup>



<sup>a</sup>The  $\Delta G_{298K}$  values were computed at the RI-BP86+D/TZVPP level for 298.15 K and  $3.3 \times 10^{-3}$  mbar. The analysis of the conformational space of Co(I) complex **6** at  $m/z$  627 showed a range of  $\Delta E = 12.3$  kcal/mol with no zero-point-energy correction added. Only the lowest-lying structures were considered for thermodynamic reaction energies and  $\Delta G$  values.

documenting the catalytic activity of the Co(I)(dppe) species. All of the experimental results were evaluated and confirmed by a thorough computational analysis of the ion structures and thermodynamic reaction energies.

Our report provides consistent experimental and theoretical evidence concerning the intrinsic properties of cationic cobalt(dppe) complexes that clearly shows Co(I) species to be the actual catalysts in gas-phase Diels–Alder reactions, a result that is also of significance for solution-phase chemistry.

#### 4. EXPERIMENTAL SECTION

**Mass Spectrometry.** MS<sup>n</sup> experiments and gas-phase IMRs were conducted on an LTQ Orbitrap hybrid instrument equipped with a heated electrospray ionization (H-ESI) source, linear ion trap (LTQ), octapole collision cell (HCD cell), and an Orbitrap mass analyzer<sup>77,78</sup> capable of measurements with high mass accuracy and elevated resolving power. For ESI-MS analysis, diluted solutions of the cobalt catalyst were introduced into the ion source via a syringe pump (flow rate 5  $\mu\text{L}/\text{min}$ ). Spray voltages were typically 2.5–3.5 kV. The ESI heater temperature was set to 50 °C and the capillary temperature to 275 °C. To generate stable spray conditions, sheath and sweep gases were used ( $\geq 99.999\%$  N<sub>2</sub>). CID experiments (collision gas helium,  $\geq 99.999\%$  He) were performed in the LTQ with a collision energy adjusted to achieve extensive fragmentations. The collision energy used depended on the selected precursor ion.<sup>64–66,71</sup> Exact masses of the precursor and product ions were measured in the Orbitrap analyzer ( $R_{\text{fwhm}} = 30,000$ ), which was externally calibrated with caffeine, trileucine, and thymopentin before and after each measurement. All of the presented ion structures are consistent with the experimentally determined exact ion masses ( $\Delta m \leq 2$  ppm) and match the theoretical isotope distributions (e.g., see Figure 2a). Data acquisition was conducted with the Tune Plus software, and for data processing and evaluation the Qualbrowser software was used.

**Synthesis of Co(II) and Co(I) Complexes.** Chemicals were used without any further purification, except for zinc iodide, which was dried under vacuum at 120 °C overnight and stored under an argon atmosphere. Tetrahydrofuran (THF) was freshly distilled from sodium and benzophenone under argon.

CoBr<sub>2</sub>(dppe) was synthesized according to a literature-known procedure<sup>79</sup> and used without further purification. For ESI-MS analysis, fragmentation experiments, and IMRs, a 10<sup>-5</sup> M solution of CoBr<sub>2</sub>(dppe) in acetonitrile was infused into the ESI source.

The in situ reduction of CoBr<sub>2</sub>(dppe) was carried out according to the literature-known protocol of the cobalt-catalyzed Diels–Alder reaction.<sup>8,60</sup> A flame-dried and argon-flushed Schlenk flask was charged with 0.1 mmol of CoBr<sub>2</sub>(dppe), 0.2 mmol of zinc powder, and 0.2 mmol of zinc iodide. THF (3 mL) was added, and the solution was stirred for 2 h at room temperature. An aliquot of the reaction solution was diluted with THF under an argon atmosphere, and the resulting 10<sup>-5</sup> M solution was immediately infused into the ESI source for MS analysis, CID experiments, and IMRs.

**Ion/Molecule Reactions and Gas-Phase Reactivity Studies of Cobalt Complex Ions.** To conduct IMRs inside the LTQ part of the mass spectrometer, the helium buffer gas supply of the LTQ was modified according to a blueprint plan established by Gronert,<sup>47,75,80</sup> O'Hair,<sup>56,62,81</sup> and Blanksby.<sup>82</sup> Neutral reagents can be injected into the helium flow via a septum using a pump-driven syringe (Figure 7). To ensure complete evaporation of the neutral reagents, an electric tape was wrapped around the stainless steel helium capillary to allow heating of the gas flow (25–140 °C). The flow rates of both the neutral reagent and the helium were measured, the latter using a commercially available gas flow meter. To avoid leakage of the gas mixture into the environment, the open-split flow divider was replaced

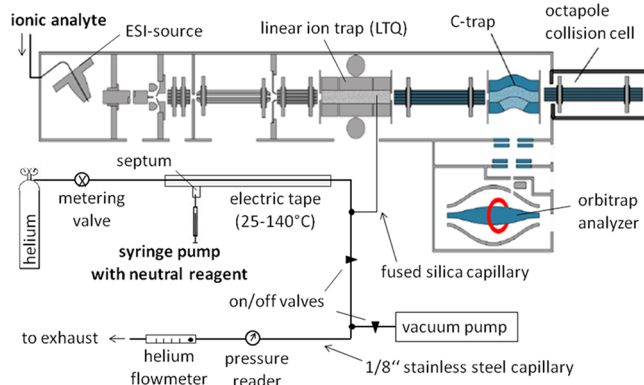


**Figure 7.** Schematic view of the modified helium buffer gas supply to an LTQ Orbitrap hybrid mass spectrometer that allows the quantity-controlled introduction of neutral reagents into the linear ion trap, LTQ (illustration reproduced and modified with the kind permission of the manufacturer).<sup>47,56,62,80,87</sup>

by a fused-silica restriction capillary (inner diameter 0.2 mm, length 25 cm), which then delivered a small fraction of the helium/neutral reagent mixture into the LTQ while most of the gas mixture ran through the gas flow meter to the exhaust placed in a fume hood. This set up required manual adjustment of the default helium pressure inside the LTQ. The experimental setup was validated using the gas-phase nucleophilic substitution of bromide anions and methyl iodide as a test reaction (Figure S9 in the SI).<sup>56,82,83</sup>

For the gas-phase reactivity studies of Co complex ions, either a single substrate or an equimolar mixture of isoprene and phenylacetylene was introduced into the helium flow (flow rates of 2.5  $\mu\text{L}/\text{min}$  for neutral reagents and 195 sL/h for helium). We note that although the neutral ratio was 1:1 at infusion, the different molar masses of isoprene and phenylacetylene cause them to effuse differently with the helium into the trap, and therefore, their ratio in the gaseous atmosphere of the trap was probably not exactly 1:1. The Co complex ions  $[\text{Co}(\text{II})\text{Br}(\text{dppe})]^+$  (1) and  $[\text{Co}(\text{I})(\text{dppe})]^+$  (2) were transferred to the gas phase by ESI-MS, monoisotopically isolated in the LTQ (isolation width 1.0 Da) and reacted with the substrates at different reaction times (30–10000 ms). The reaction time is defined as the time period between isolation of a specific ion in the LTQ and axial ejection of all of the ions from the trap for analysis. Prior to each experiment, a delay time of typically 10–20 min was kept to ensure constant-concentration conditions of neutral reagents inside the trap (i.e., no observable change of the precursor ion/adduct ion ratio at a specific reaction time).

All of the IMRs were performed without applying any additional collision activation energy. As experimental and theoretical experiments have documented, ions stored in linear as well as in spherical quadrupole ion traps are effectively thermalized by multiple collisions with the surrounding helium buffer gas atoms. Stored ions therefore exhibit a Boltzmann energy distribution as the rapid energy exchange with the buffer gas outweighs the impact of the electric field of the trap on the internal energy of the ions.<sup>47,84–86</sup> Hence, the ion trap environment allows the investigation of quasi-thermal IMRs.<sup>75,76</sup>

**Quantum-Chemical Calculations.** Geometry optimizations of the molecules were carried out using the DFT functional BP86<sup>88,89</sup> with def2-TZVPP basis sets.<sup>90,91</sup> The RI approximation was applied using auxiliary basis functions.<sup>92–95</sup> Grimme's DFTD3 dispersion correction with Becke–Johnson damping was included.<sup>96–100</sup> This level of theory is denoted as RI-BP86+D/TZVPP. The optimized geometries were verified as minima on the potential energy surface by calculation of the vibrational frequencies analytically at the RI-BP86+D/TZVPP level of theory (AOFORCE).<sup>101–103</sup>

## ■ ASSOCIATED CONTENT

### ● Supporting Information

Kinetic data for the gas-phase test reaction, additional mass spectra of CID experiments, and experimental and theoretical data for IMRs. This material is available free of charge via the Internet at <http://pubs.acs.org>.

## ■ AUTHOR INFORMATION

### Corresponding Author

\*Tel: +49-221-470-3086. E-mail: [mathias.schaefer@uni-koeln.de](mailto:mathias.schaefer@uni-koeln.de).

### Notes

The authors declare no competing financial interest.

## ■ ACKNOWLEDGMENTS

This work was generously supported by a doctoral fellowship of the "Cusanuswerk" to L.F. L.F. gratefully acknowledges Mark Davis (Virginia Commonwealth University, Richmond, VA) and Dr. George N. Khairallah (University of Melbourne, Australia) for helpful discussions regarding the design of instrument modifications and kinetic analyses.

## ■ REFERENCES

- (1) Diels, O.; Alder, K. *Liebigs Ann. Chem.* **1928**, *60*, 98.
- (2) Fringuelli, F.; Taticchi, A. *The Diels–Alder Reaction*; Wiley-VCH: New York, 2001.
- (3) Nicolaou, K. C.; Snyder, S. A.; Montagnon, T.; Vassilikogiannakis, G. *Angew. Chem., Int. Ed.* **2002**, *41*, 1668.
- (4) Paik, S. J.; Son, S. U.; Chung, Y. K. *Org. Lett.* **1999**, *1*, 2045.
- (5) Wang, B.; Cao, P.; Zhang, X. M. *Tetrahedron Lett.* **2000**, *41*, 8041.
- (6) Lee, S. I.; Park, Y.; Park, J. H.; Jung, G.; Choi, S. Y.; Chung, Y. K.; Lee, B. Y. *J. Org. Chem.* **2006**, *71*, 91.
- (7) Aikawa, K.; Akutagawa, S.; Mikami, K. *J. Am. Chem. Soc.* **2006**, *128*, 12648.
- (8) Hilt, G.; Janikowski, J.; Hess, W. *Angew. Chem., Int. Ed.* **2006**, *45*, 5204.
- (9) Fürstner, A.; Stimson, C. C. *Angew. Chem., Int. Ed.* **2007**, *46*, 8845.
- (10) Shintani, R.; Sannohe, Y.; Tsuji, T.; Hayashi, T. *Angew. Chem., Int. Ed.* **2007**, *46*, 7277.
- (11) Hilt, G.; Janikowski, J. *Org. Lett.* **2009**, *11*, 773.
- (12) Arndt, M.; Dindaroglu, M.; Schmalz, H.-G.; Hilt, G. *Org. Lett.* **2011**, *13*, 6236.
- (13) Hilt, G.; Roesner, S. *Synthesis* **2011**, 662.
- (14) Hilt, G. *Eur. J. Org. Chem.* **2012**, 4441.
- (15) Hilt, G.; Vogler, T.; Hess, W.; Galbiati, F. *Chem. Commun.* **2005**, 1474.
- (16) Hilt, G.; Hess, W.; Vogler, T.; Hengst, C. *J. Organomet. Chem.* **2005**, *690*, 5170.
- (17) Hilt, G.; Treutwein, J. *Angew. Chem., Int. Ed.* **2007**, *46*, 8500.
- (18) Hilt, G.; Erver, F.; Harms, K. *Org. Lett.* **2011**, *13*, 304.
- (19) Erver, F.; Hilt, G. *J. Org. Chem.* **2012**, *77*, 5215.
- (20) Hilt, G.; Janikowski, J. *Angew. Chem.* **2008**, *120*, 5321.
- (21) Treutwein, J.; Hilt, G. *Angew. Chem., Int. Ed.* **2008**, *47*, 6811.
- (22) Hilt, G.; du Mesnil, F.-X. *Tetrahedron Lett.* **2000**, *41*, 6757.
- (23) Ma, B.; Snyder, J. K. *Org. Lett.* **2002**, *4*, 2731.
- (24) Pünner, F.; Schmidt, A.; Hilt, G. *Angew. Chem., Int. Ed.* **2012**, *51*, 1270.
- (25) Hilt, G.; Hengst, C.; Arndt, M. *Synthesis* **2009**, 395.
- (26) Pünner, F.; Hilt, G. *Chem. Commun.* **2012**, 48, 3617.
- (27) Mörschel, P.; Janikowski, J.; Hilt, G.; Frenking, G. *J. Am. Chem. Soc.* **2008**, *130*, 8952.
- (28) Fenn, J. B.; Mann, M.; Meng, C. K.; Wong, S. F.; Whitehouse, C. M. *Science* **1989**, *246*, 64.
- (29) Cole, R. *Electrospray Ionization Mass Spectrometry: Fundamentals, Instrumentation and Applications*; Wiley: New York, 1997.
- (30) Kebarle, P.; Verkerk, U. H. *Mass Spectrom. Rev.* **2009**, *28*, 898.
- (31) Wells, J. M.; McLuckey, S. A. *The Encyclopedia of Mass Spectrometry*; Elsevier: New York, 2003; Vol. 1.
- (32) Aliprantis, A. O.; Canary, J. W. *J. Am. Chem. Soc.* **1994**, *116*, 6985.
- (33) Guo, H.; Qian, R.; Liao, Y. X.; Ma, S. M.; Guo, Y. L. *J. Am. Chem. Soc.* **2005**, *127*, 13060.
- (34) Santos, L. S.; Rosso, G. B.; Pilli, R. A.; Eberlin, M. N. *J. Org. Chem.* **2007**, *72*, 5809.
- (35) Markert, C.; Neuburger, M.; Kulicke, K.; Meuwly, M.; Pfaltz, A. *Angew. Chem., Int. Ed.* **2007**, *46*, 5892.
- (36) Fernandes, T. D.; Vaz, B. G.; Eberlin, M. N.; da Silva, A. J. M.; Costa, P. R. R. *J. Org. Chem.* **2010**, *75*, 7085.
- (37) Vikse, K. L.; Henderson, M. A.; Oliver, A. G.; McIndoe, J. S. *Chem. Commun.* **2010**, 46, 7412.
- (38) Schade, M. A.; Fleckenstein, J. E.; Knochel, P.; Koszinowski, K. *J. Org. Chem.* **2010**, *75*, 6848.
- (39) Fiebig, L.; Schmalz, H.-G.; Schäfer, M. *Int. J. Mass Spectrom.* **2011**, *308*, 307.
- (40) Coelho, F.; Eberlin, M. N. *Angew. Chem., Int. Ed.* **2011**, *50*, 5261.
- (41) Vikse, K. L.; Ahmadi, Z.; Manning, C. C.; Harrington, D. A.; McIndoe, J. S. *Angew. Chem., Int. Ed.* **2011**, *50*, 8304.
- (42) Putau, A.; Brand, H.; Koszinowski, K. *J. Am. Chem. Soc.* **2012**, *134*, 613.



- (43) Santos, L. S.; Knaack, L.; Metzger, J. O. *Int. J. Mass Spectrom.* **2005**, *246*, 84.
- (44) Eberlin, M. N. *Eur. J. Mass Spectrom.* **2007**, *13*, 19.
- (45) Santos, L. S. *Eur. J. Org. Chem.* **2008**, 235.
- (46) Eller, K.; Schwarz, H. *Chem. Rev.* **1991**, *91*, 1121.
- (47) Gronert, S. *Mass Spectrom. Rev.* **2005**, *24*, 100.
- (48) Operti, L.; Rabezzana, R. *Mass Spectrom. Rev.* **2006**, *25*, 483.
- (49) O'Hair, R. A. J. *Chem. Commun.* **2006**, 1469.
- (50) Wang, L. C.; Jang, H. Y.; Roh, Y.; Lynch, V.; Schultz, A. J.; Wang, X. P.; Krische, M. J. *J. Am. Chem. Soc.* **2002**, *124*, 9448.
- (51) Combariza, M. Y.; Fahey, A. M.; Milshcheyn, A.; Vachet, R. W. *Int. J. Mass Spectrom.* **2005**, *244*, 109.
- (52) Combariza, M. Y.; Vachet, R. W. *J. Am. Soc. Mass Spectrom.* **2002**, *13*, 813.
- (53) Innorta, G.; Pontoni, L.; Torroni, S. *J. Am. Soc. Mass Spectrom.* **1998**, *9*, 314.
- (54) Innorta, G.; Torroni, S.; Maranzana, A.; Tonachini, G. *J. Organomet. Chem.* **2001**, *626*, 24.
- (55) Innorta, G.; Torroni, S.; Basili, F.; Di Fabio, A. *J. Organomet. Chem.* **2002**, *650*, 69.
- (56) Waters, T.; O'Hair, R. A. J.; Wedd, A. G. *J. Am. Chem. Soc.* **2003**, *125*, 3384.
- (57) Plattner, D. A. *Int. J. Mass Spectrom.* **2001**, *207*, 125.
- (58) Chen, P. *Angew. Chem., Int. Ed.* **2003**, *42*, 2832.
- (59) Santos, L. S.; Metzger, J. O. *Angew. Chem., Int. Ed.* **2006**, *45*, 977.
- (60) Arndt, M.; Hilt, G.; Khlebnikov, A. F.; Kozhushkov, S. I.; de Meijere, A. *Eur. J. Org. Chem.* **2012**, 3112.
- (61) Lemr, K.; Holcapek, M.; Jandera, P. *Rapid Commun. Mass Spectrom.* **2000**, *14*, 1878.
- (62) Donald, W. A.; McKenzie, C. J.; O'Hair, R. A. J. *Angew. Chem.* **2011**, *123*, 8529.
- (63) The natural log plots of relative parent ion intensity versus time showed nonlinear behavior, indicating that pseudo-first order kinetics were not being obeyed. However, when precursor ion 2 was reselected at late reaction times in the IMR with phenylacetylene, a linear natural log plot was obtained, pointing to the presence of two isomers of 2 with different reactivities toward phenylacetylene (Figure S3b in the SI).
- (64) Thermo Scientific Product Support Bulletin 104. [http://www.thermoscientific.de/eThermo/CMA/PDFs/Articles/articlesFile\\_21418.pdf](http://www.thermoscientific.de/eThermo/CMA/PDFs/Articles/articlesFile_21418.pdf) (accessed Sept 25, 2013).
- (65) Borisov, O. V.; Goshe, M. B.; Conrads, T. P.; Rakov, V. S.; Veenstra, T. D.; Smith, R. D. *Anal. Chem.* **2002**, *74*, 2284.
- (66) Revesz, A.; Milko, P.; Zabka, J.; Schröder, D.; Roithova, J. *J. Mass Spectrom.* **2010**, *45*, 1246.
- (67) Hinderling, C.; Adlhart, C.; Chen, P. *Angew. Chem., Int. Ed.* **1998**, *37*, 2685.
- (68) Sabino, A. A.; Machado, A. H. L.; Correia, C. R. D.; Eberlin, M. N. *Angew. Chem., Int. Ed.* **2004**, *43*, 2514.
- (69) March, R. E. *Mass Spectrom. Rev.* **2009**, *28*, 961.
- (70) Senko, M. W.; Cunniff, J. B.; Land, A. P. Presented at the 46th ASMS Conference on Mass Spectrometry and Allied Topics, Orlando, FL, May 31–June 4, 1998; paper 486.
- (71) Lopez, L. L.; Tiller, P. R.; Senko, M. W.; Schwartz, J. C. *Rapid Commun. Mass Spectrom.* **1999**, *13*, 663.
- (72) Wysocki, V. H.; Kenttämaa, H. I.; Cooks, R. G. *Int. J. Mass Spectrom. Ion Processes* **1987**, *75*, 181.
- (73) Cooks, R. G.; Kaiser, R. E. *Acc. Chem. Res.* **1990**, *23*, 213.
- (74) The calculations in ref 27 were done with a smaller basis set (def2-SVP) than used in this work. Recalculation of the reaction step for the 6 → 6' interconversion at the BP86/def2-TZVPP level gave a very similar value of 10.9 kcal/mol for the free energy barrier.
- (75) Gronert, S. *J. Am. Soc. Mass Spectrom.* **1998**, *9*, 845.
- (76) Donald, W. A.; Khairallah, G. N.; O'Hair, R. A. J. *J. Am. Soc. Mass Spectrom.* **2013**, *24*, 811.
- (77) Makarov, A. *Anal. Chem.* **2000**, *72*, 1156.
- (78) Makarov, A.; Denisov, E.; Kholomeev, A.; Baischun, W.; Lange, O.; Strupat, K.; Horning, S. *Anal. Chem.* **2006**, *78*, 2113.
- (79) Hilt, G.; Lüers, S. *Synthesis* **2002**, 609.
- (80) Flores, A. E.; Gronert, S. *J. Am. Chem. Soc.* **1999**, *121*, 2627.
- (81) Robinson, P. S. D.; Khairallah, G. N.; da Silva, G.; Lioe, H.; O'Hair, R. A. J. *Angew. Chem.* **2012**, *124*, 3878.
- (82) Harman, D. G.; Blanksby, S. J. *Org. Biomol. Chem.* **2007**, *5*, 3495.
- (83) Gronert, S.; Depuy, C. H.; Bierbaum, V. M. *J. Am. Chem. Soc.* **1991**, *113*, 4009.
- (84) Butschke, B.; Schwarz, H. *Int. J. Mass Spectrom.* **2011**, *306*, 108.
- (85) Schröder, D.; Schwarz, H.; Schenk, S.; Anders, E. *Angew. Chem., Int. Ed.* **2003**, *42*, 5087.
- (86) Schröder, D.; Engeser, M.; Schwarz, H.; Rosenthal, E. C. E.; Dobler, J.; Sauer, J. *Inorg. Chem.* **2006**, *45*, 6235.
- (87) *LTQ Orbitrap XL Hardware Manual*; Thermo Fisher Scientific: Bremen, Germany, 2007.
- (88) Becke, A. D. *Phys. Rev. A* **1988**, *38*, 3098.
- (89) Perdew, J. P. *Phys. Rev. B* **1986**, *33*, 8822.
- (90) Schäfer, A.; Horn, H.; Ahlrichs, R. *J. Chem. Phys.* **1992**, *97*, 2571.
- (91) Weigend, F.; Haser, M.; Patzelt, H.; Ahlrichs, R. *Chem. Phys. Lett.* **1998**, *294*, 143.
- (92) Ahlrichs, R. *Phys. Chem. Chem. Phys.* **2004**, *6*, 5119.
- (93) Eichkorn, K.; Treutler, O.; Ohm, H.; Haser, M.; Ahlrichs, R. *Chem. Phys. Lett.* **1995**, *242*, 652.
- (94) Eichkorn, K.; Weigend, F.; Treutler, O.; Ahlrichs, R. *Theor. Chem. Acc.* **1997**, *97*, 119.
- (95) Weigend, F. *Phys. Chem. Chem. Phys.* **2006**, *8*, 1057.
- (96) Grimme, S. *J. Comput. Chem.* **2006**, *27*, 1787.
- (97) Grimme, S.; Antony, J.; Ehrlich, S.; Krieg, H. *J. Chem. Phys.* **2010**, *132*, No. 154104.
- (98) Becke, A. D.; Johnson, E. R. *J. Chem. Phys.* **2005**, *122*, No. 154104.
- (99) Johnson, E. R.; Becke, A. D. *J. Chem. Phys.* **2005**, *123*, No. 024101.
- (100) Johnson, E. R.; Becke, A. D. *J. Chem. Phys.* **2006**, *124*, No. 174104.
- (101) Deglmann, P.; Furche, F. *J. Chem. Phys.* **2002**, *117*, 9535.
- (102) Deglmann, P.; Furche, F.; Ahlrichs, R. *Chem. Phys. Lett.* **2002**, *362*, 511.
- (103) Deglmann, P.; May, K.; Furche, F.; Ahlrichs, R. *Chem. Phys. Lett.* **2004**, *384*, 103.